

Complex Heavy Quarkonium Potential in an Anisotropic Collisional Quark-Gluon Plasma

Manas Debnath, ^{1,*} Lata Thakur, ^{2,†} and Najmul Haque, ^{1,‡}

¹*School of Physical Sciences, National Institute of Science Education and Research,
An OCC of Homi Bhabha National Institute,
Jatni, Khurda 752050, India*

²*Department of Physics and Institute of Physics and Applied Physics, Yonsei University,
Seoul 03722, Korea*

arXiv:2504.02802v1 [hep-ph] 3 Apr 2025

Abstract

We compute the complex heavy-quark potential in an anisotropic quark-gluon plasma (QGP) using kinetic theory with a Bhatnagar-Gross-Krook (BGK) collision kernel to incorporate collisions via gluon collective modes. By modifying the medium's dielectric permittivity with momentum anisotropy and finite collisional rates, we derive both the real and imaginary components of the potential. While collisions have minimal impact on the real part and binding energy, they significantly amplify the imaginary part, modulating the effects of anisotropy. This enhancement increases quarkonium dissociation rates in a nonequilibrium QGP, offering deeper insights into suppression mechanisms.

Keywords: Heavy quarkonium, Quantum chromodynamics, Momentum anisotropy, Collisional plasma.

I. INTRODUCTION

The study of the quark-gluon plasma (QGP) is a central focus of current experiments at the Relativistic Heavy Ion Collider (RHIC) at Brookhaven National Laboratory (BNL) and at the Large Hadron Collider (LHC) at CERN. These experiments aim to uncover the properties of QGP, a state of matter that is expected to emerge at extremely high temperatures, where quarks and gluons exist in a deconfined state. At sufficiently high temperatures, QGP exhibits the behavior of a weakly interacting system, a feature that can be understood through hard thermal loop (HTL) resummation techniques [1–6].

Heavy quarkonium suppression serves as a crucial signal for the presence of QGP [7]. In a vacuum, quarkonium states are well characterized by non-relativistic potential models, which exhibit a Coulomb-like behavior at short distances and a linear confining potential at larger distances [8–13]. However, in a hot medium, the quark-antiquark potential is modified due to Debye screening, leading to the dissociation of quarkonium bound states above the crossover temperature [7]. The quarkonium states' binding energy ranges from a few MeV to a few GeV, which could result in a “sequential suppression” [14] as the weakly bound states melt near transition temperature, and the more tightly bound states melt at higher temperature. This sequential melting of quarkonium states has been observed in experiments at RHIC and LHC, where higher-mass states of bottomonia and charmonia [15, 16] exhibit stronger suppression.

While earlier studies of heavy quarkonium in QGP assume an isotropic medium [17], the early stages of heavy-ion collisions introduce momentum-space anisotropies caused by the rapid expansion of the plasma [18–20]. Non-central collisions, in particular, generate an anisotropic momentum distribution, leading to differential pressures in longitudinal and transverse directions, resulting in a momentum space anisotropy, and it causes a kinetic instability [21]. The instability has a significant effect on the system's evolution, leading to faster isotropization [21, 22]. This anisotropy influences collective gluon modes [18, 23], which in turn modify the heavy-quark potential [23–28]. In addition to the momentum anisotropy, the collisions among plasma constituents are usually ignored at high temperatures as the hard collision (large momentum exchange) time scale is much longer than the time scale for the soft momentum exchange [29]. When the temperature of the system decreases, it becomes necessary to consider both hard and soft collisions.

The gluon collective modes in an isotropic thermal QGP with collisional effects have been studied using a Bhatnagar-Gross-Krook (BGK) collisional kernel [30], and this formalism has been extended to anisotropic plasmas [31] in which the authors have considered only those modes which are propagating parallel to the anisotropy vector. In Ref. [31], the authors found a single unstable mode and a few other stable modes. Later, in Ref. [32], the authors considered the modes that can propagate in all possible directions with respect to the (small) anisotropy vector, where they considered the interacting medium in terms of the effective quasiparticle model. Recently, in Ref. [29], the authors extended the existing results for the collective modes by incorporating the full angular dependence of gluon propagation while considering general anisotropy strength.

Previous studies have explored quarkonium properties in an anisotropic QGP under collisionless scenarios [23, 24, 27, 33], while Ref. [29] examined collective modes with collisions. In this work, we extend these efforts by systematically deriving the complex heavy-quark potential in a momentum-anisotropic QGP with finite collisional effects. Using the collective modes of Ref. [29], for the first time, we compute the real and imaginary components of the potential, incorporating both general anisotropy and the BGK collision kernel. Our studies reveal how these effects influence quarkonium thermal widths and dissociation rates in a nonequilibrium QGP, providing valuable insights into quarkonium suppression in relativistic heavy-ion collisions.

* manas.debnath@niser.ac.in

† thakurphyom@gmail.com

‡ nhaque@niser.ac.in

In addition to the quarkonium potential in an anisotropy system, the quarkonium properties are also studied in various non-trivial situations relevant to HIC. As a strong magnetic field appears in non-central HIC, the heavy quarkonium properties are studied in the presence of an external magnetic field [34, 35]. Additionally, the quarkonium properties are also studied when there is relative motion between the medium and quarkonium [36, 37] and in a bulk viscous medium [38, 39].

The paper is structured as follows: Section II discusses the gluon propagator in a collisional anisotropic QGP medium. In Section III, we discuss the dielectric permittivity of the collisional anisotropic QGP medium. In section IV, we present the derivation of the complex heavy-quark potential and examine the impact of collisions and momentum-anisotropy on the real and imaginary components of the potential. In Section V, we study the thermal width of the ground state of charmonium. Finally, we summarize our results and discuss their implications in Section VI.

II. GLUON PROPAGATOR IN A COLLISIONAL ANISOTROPIC MEDIUM

In this section, we discuss the gluon self-energy and propagator in the presence of a collisional anisotropic QGP medium, which we later use to compute the permittivity of the medium and eventually use that to determine the in-medium heavy quark-antiquark potential.

The momentum-space anisotropic correction is introduced by deforming the distribution functions of constituent particles [18]. The deformed distribution function is parametrized in the following spheroidal form

$$\begin{aligned} f(\mathbf{k}) &= f_{\text{iso}} \left(\frac{1}{\lambda} \sqrt{k_T^2 + (1 + \xi)k_L^2} \right) \\ &= f_{\text{iso}} \left(\frac{1}{\lambda} \sqrt{\mathbf{k}^2 + \xi(\mathbf{k} \cdot \mathbf{n})^2} \right), \end{aligned} \quad (1)$$

where $f(\mathbf{k})$ is derived from $f_{\text{iso}}(k)$ by filtering out particles with a large momentum component along the anisotropic direction, \mathbf{n} [18]. Here, k_T and k_L denote the components of momentum transverse and longitudinal to a given anisotropy axis \mathbf{n} with $k = |\mathbf{k}| = \sqrt{k_T^2 + k_L^2}$. Here, in Eq. (1), the parameter ξ quantitatively measures the strength of momentum-space anisotropy. The quantity λ serves as a typical characteristic momentum scale of plasma particles. Here, it is relevant as the temperature is only in thermal equilibrium. Considering a spheroidal distortion, only one anisotropy axis is being considered. As a result, the modes of the gluon polarization tensor depend on the propagation angle relative to \mathbf{n} . We first calculate the gluon self-energy and propagators in a collisional anisotropic QGP medium. Subsequently, we determine the inverse dielectric permittivity of the anisotropic medium with collision, which will be used to compute the real and imaginary parts of the quarkonium static potential.

A. Gluon self-energy and resummed propagator

In the collisionless case, the gluon self-energy is typically obtained by the hard thermal loop (HTL) resummation technique from the Feynman diagrams. However, for the collisional QGP, the gluon self-energy is usually obtained using the Kinetic theory [29–31]. Within the framework of kinetic theory, the phase-space distribution of partons (viz. gluons, quarks, and antiquarks) in the QCD plasma is characterized using gauge-covariant Wigner functions, $W^i(\mathbf{k}, X)$ with $i \in \{g, q, \bar{q}\}$ and \mathbf{k} and X denote the three momentum and four position respectively. These particles are treated as massless and satisfy the mass-shell constraint. To obtain the linearized transport equation, we expand $W^i(\mathbf{k}, X) = W^i(\mathbf{k}) + \delta W^i(\mathbf{k}, X)$. After applying a gauge-covariant gradient expansion, the generalized Boltzmann equation governing quarks and gluons takes the form

$$V \cdot \partial_X \delta f_a^i(\mathbf{k}, X) + g\theta_i V_\mu F_a^{\mu\nu} \partial_\nu^{(K)} f^i(\mathbf{k}) = C_a^i(\mathbf{k}, X), \quad (2)$$

where $V = (1, \mathbf{v})$ with $\mathbf{v} \equiv \mathbf{k}/k$ and $\theta_g = \theta_q = 1, \theta_{\bar{q}} = -1$. In Eq. (2), the weak-coupling limit is taken, and higher order terms of coupling g are neglected. So the field tensor becomes $F^{\mu\nu} = \partial_\mu A_\nu - \partial_\nu A_\mu + \mathcal{O}(g)$. In this limit, the theory becomes effectively Abelian, and one may consider there is no coupling between different color channels. The distribution function $f^i(\mathbf{k})$ and its color fluctuations $\delta f_a^i(\mathbf{k}, X)$ are related via the Wigner function as

$$f^{q/\bar{q}}(\mathbf{k}) = \frac{1}{N_c} \text{Tr}[W^{q/\bar{q}}(\mathbf{k}, X)], \quad f^g(\mathbf{k}) = \frac{1}{N_c^2 - 1} \text{Tr}[W^g(\mathbf{k}, X)], \quad (3)$$

and

$$\delta f_a^{q/\bar{q}}(\mathbf{k}, X) = 2 \text{Tr}[t_a \delta W^{q/\bar{q}}(\mathbf{k}, X)], \quad \delta f_a^g(\mathbf{k}, X) = \frac{1}{N_c} \text{Tr}[T_a \delta W^g(\mathbf{k}, X)], \quad (4)$$

where t_a is the $SU(N_c)$ group generators in the fundamental representation and T_a is the corresponding adjoint representations. Now, for the collisionless case, the right-hand side of Eq. (2) is simply zero, that is, $C_a^i(\mathbf{k}, X) = 0$. But when we include collision, $C_a^i(\mathbf{k}, X)$ can be given by a BGK-type collision kernel,

$$C_a^i(\mathbf{k}, X) = -\nu \left[f_a^i(\mathbf{k}, X) - \frac{N_a^i(X)}{N_{eq}^i} f_{eq}^i(k) \right], \quad (5)$$

with $f_a^i(\mathbf{k}, X) = f^i(\mathbf{k}) + \delta f_a^i(\mathbf{k}, X)$, and

$$N_a^i(X) = \int_{\mathbf{k}} f_a^i(\mathbf{k}, X), \quad N_{eq}^i = \int_{\mathbf{k}} f_{eq}^i(k). \quad (6)$$

The BGK-type collision term in Eq. (5) characterizes the equilibration of the system through collisions, occurring over a timescale inversely proportional to ν . In this work, the collision parameter, ν , is taken to be a free parameter, with no dependence on particle momentum and particle species. The advantage of the BGK kernel is that the particle number conservation is instantaneously followed; that is,

$$\int_{\mathbf{k}} C_a^i(\mathbf{k}, X) = 0. \quad (7)$$

In Ref. [31], it is estimated that ν lies in the range $\nu \sim 0.1m_D - 0.2m_D$, but it is possible that the collision rate could even be larger than this. However, in this article, we have assumed a small ν . The induced current for each color channel is given by,

$$J_{ind,a}^\mu = g \int_{\mathbf{k}} V^\mu \{ 2N_c \delta f_a^g(k, X) + N_f [\delta f_a^q(k, X) - \delta f_a^{\bar{q}}(k, X)] \}. \quad (8)$$

The gluon self-energy for the collisional case can be obtained following the Ref. [29, 31] as

$$\begin{aligned} \Pi_{ab}^{\mu\nu}(P) &= \frac{\delta J_{ind,a}^\mu(P)}{\delta A_\nu^b(P)} \\ &= g^2 \delta_{ab} \int_{\mathbf{k}} V^\mu \partial_l^{\mathbf{k}} f(\mathbf{k}) \frac{g^{l\nu}(\hat{\omega} - \hat{\mathbf{p}} \cdot \mathbf{v}) - \hat{P}^l V^\nu}{\hat{\omega} - \hat{\mathbf{p}} \cdot \mathbf{v} + i\hat{\nu}} + g^2 \delta_{ab} (i\hat{\nu}) \int \frac{d\Omega}{4\pi} \frac{V^\mu}{\hat{\omega} - \hat{\mathbf{p}} \cdot \mathbf{v} + i\hat{\nu}} \\ &\times \int_{\mathbf{k}'} \partial_l^{\mathbf{k}'} f(\mathbf{k}') \frac{g^{l\nu}(\hat{\omega} - \hat{\mathbf{p}} \cdot \mathbf{v}') - \hat{P}^l V^\nu}{\hat{\omega} - \hat{\mathbf{p}} \cdot \mathbf{v}' + i\hat{\nu}} \mathcal{W}^{-1}(\hat{\omega}, \hat{\nu}), \end{aligned} \quad (9)$$

where $\int_{\mathbf{k}} \equiv \int d^3\mathbf{k}/(2\pi)^3$. For convenience, we define the dimensionless collision rate $\hat{\nu} = \nu/p$. $\hat{P} = (\hat{\omega}, \hat{\mathbf{p}})$ with $\hat{\omega} = \omega/p$ and $\hat{\mathbf{p}} = \mathbf{p}/p$. The function $\mathcal{W}(\hat{\omega}, \hat{\nu})$ is defined as

$$\mathcal{W}(\hat{\omega}, \hat{\nu}) = 1 - \frac{i\hat{\nu}}{2} \int_{-1}^1 \frac{dy}{\hat{\omega} - y + i\hat{\nu}} = 1 - \frac{i\hat{\nu}}{2} \ln \frac{\hat{\omega} + i\hat{\nu} + 1}{\hat{\omega} + i\hat{\nu} - 1}. \quad (10)$$

In Eq. (9), $f(\mathbf{k}) = N_f [f^q(\mathbf{k}) + f^{\bar{q}}(\mathbf{k})] + N_c f^g(\mathbf{k})$, where the distribution function of partons is anisotropic as defined in eq. (1). The gluon self-energy still satisfied the transversality condition even after introducing the collisional term. The spatial component of gluon self-energy can be obtained after substituting the Eq. (1) into Eq. (9) as

$$\begin{aligned} \Pi^{ij}(P) &= m_D^2 \int \frac{d\Omega}{4\pi} v^i \frac{v^l + \xi(\mathbf{v} \cdot \mathbf{n})n^l}{(1 + \xi(\mathbf{v} \cdot \mathbf{n})^2)^2} \frac{\delta^{lj}(\hat{\omega} - \hat{\mathbf{p}} \cdot \mathbf{v}) + \hat{p}^l v^j}{\hat{\omega} - \hat{\mathbf{p}} \cdot \mathbf{v} + i\hat{\nu}} + i\hat{\nu} m_D^2 \int \frac{d\Omega'}{4\pi} \frac{v'^i}{\hat{\omega} - \hat{\mathbf{p}} \cdot \mathbf{v}' + i\hat{\nu}} \\ &\times \int \frac{d\Omega}{4\pi} \frac{v^l + \xi(\mathbf{v} \cdot \mathbf{n})n^l}{(1 + \xi(\mathbf{v} \cdot \mathbf{n})^2)^2} \frac{\delta^{lj}(\hat{\omega} - \hat{\mathbf{p}} \cdot \mathbf{v}) + \hat{p}^l v^j}{\hat{\omega} - \hat{\mathbf{p}} \cdot \mathbf{v} + i\hat{\nu}} \mathcal{W}(\hat{\omega}, \hat{\nu})^{-1}, \end{aligned} \quad (11)$$

where

$$m_D^2 = -\frac{g^2}{2\pi^2} \int_0^\infty dk k^2 \frac{df_{iso}(k)}{dk}. \quad (12)$$

The gluon self-energy given in Eq. (11) is asymmetric in the Lorentz indices due to the presence of a collision term of BGK-type. This asymmetry is also seen in magnetized plasma because of the lack of time-reversal symmetry [40].

Therefore, the symmetric tensor basis for anisotropic systems in the collisionless limit is unsuitable for the decomposition in in Eq. (11). Instead, we adopt a more general tensor basis with five structure functions to decompose the gluon self-energy.

$$\Pi^{ij}(P) = \alpha A^{ij} + \beta B^{ij} + \gamma C^{ij} + \delta D^{ij} + \rho E^{ij}, \quad (13)$$

with the tensor basis defined as

$$A^{ij} = \delta^{ij} - \hat{p}^i \hat{p}^j, \quad B^{ij} = \hat{p}^i \hat{p}^j, \quad C^{ij} = \frac{\tilde{n}^i \tilde{n}^j}{\tilde{n}^2}, \quad D^{ij} = \tilde{n}^i \hat{p}^j, \quad E^{ij} = \tilde{n}^j \hat{p}^i \quad (14)$$

Here, $\tilde{n}^i \equiv A^{ij} n^j$, which is orthogonal to \hat{p}^i . Note that the basis functions follow the following orthonormal conditions:

$$A^{ij} A^{ij} = 2, \quad B^{ij} B^{ij} = 1, \quad C^{ij} C^{ij} = 1, \quad D^{ij} D^{ij} = 0, \quad E^{ij} E^{ij} = 0, \quad (15a)$$

$$\hat{p}^i A^{ij} = 0, \quad \hat{p}^i B^{ij} = \hat{p}^j, \quad \hat{p}^i C^{ij} = 0, \quad \hat{p}^i D^{ij} = 0, \quad \hat{p}^i E^{ij} = \tilde{n}^j, \quad (15b)$$

$$\tilde{n}^i A^{ij} = \tilde{n}^j, \quad \tilde{n}^i B^{ij} = 0, \quad \tilde{n}^i C^{ij} = \tilde{n}^j, \quad \tilde{n}^i D^{ij} = \tilde{n}^2 \hat{p}^j, \quad \tilde{n}^i E^{ij} = 0. \quad (15c)$$

Using the orthonormal properties of the tensor basis, the five structure functions can be determined from Eq. (13) based on the following contraction as

$$\hat{p}^i \Pi^{ij} \hat{p}^j = \beta, \quad (16a)$$

$$\tilde{n}^i \Pi^{ij} \tilde{n}^j = \tilde{n}^2 (\alpha + \gamma), \quad (16b)$$

$$\tilde{n}^i \Pi^{ij} \hat{p}^j = \tilde{n}^2 \delta, \quad (16c)$$

$$\hat{p}^i \Pi^{ij} \tilde{n}^j = \tilde{n}^2 \rho, \quad (16d)$$

$$\text{Tr} \Pi^{ij} = 2\alpha + \beta + \gamma. \quad (16e)$$

By utilizing gluon self-energy, the inverse of the resummed gluon propagator $\Delta^{ij}(P)$ can be computed in temporal axial gauge using the Dyson-Schwinger equation as

$$(\Delta^{-1})^{ij}(P) = (p^2 - \omega^2 + \alpha) A^{ij} + (\beta - \omega^2) B^{ij} + \gamma C^{ij} + \delta D^{ij} + \rho E^{ij}. \quad (17)$$

Upon inversion, the resummed gluon propagator becomes

$$\Delta^{ij}(P) = \Delta_A [A^{ij} - C^{ij}] + \Delta_G [(p^2 - \omega^2 + \alpha + \gamma) B^{ij} + (\beta - \omega^2) C^{ij} - \delta D^{ij} - \rho E^{ij}], \quad (18)$$

with

$$\Delta_A = \frac{1}{\omega^2 - p^2 - \alpha},$$

$$\Delta_G = \frac{1}{(p^2 - \omega^2 + \alpha + \gamma)(\beta - \omega^2) - \tilde{n}^2 \delta \rho}. \quad (19)$$

The dispersion relation can be determined by finding the poles of the propagator $\Delta^{ij}(P)$, namely,

$$\Delta_A^{-1} = \omega^2 - p^2 - \alpha = 0,$$

$$\Delta_G^{-1} = (p^2 - \omega^2 + \alpha + \gamma)(\beta - \omega^2) - \tilde{n}^2 \delta \rho = (\omega^2 - \Omega_+^2)(\omega^2 - \Omega_-^2) = 0, \quad (20)$$

where

$$2\Omega_\pm^2 = \bar{\Omega}^2 \pm \sqrt{\bar{\Omega}^4 - 4[(\alpha + \gamma + p^2)\beta - \tilde{n}^2 \delta \rho]}, \quad (21)$$

with

$$\bar{\Omega}^2 = \alpha + \beta + \gamma + p^2. \quad (22)$$

From Eq. (16), we can get the following forms of the structure functions ([29]),

$$\alpha(\xi, \hat{\omega}, t, \hat{\nu}) = \frac{m_D^2}{2(1-t^2)} \left[\hat{\omega} z f_0(\xi) - \xi t^2 f_1(\xi) + \hat{\omega}(1-t^2-z^2) \mathcal{I}^{[0]}(\xi, \hat{\omega}, t, \hat{\nu}) \right. \\ \left. + t \{ \xi(1-t^2) + z(2\hat{\omega} - \xi z) \} \mathcal{I}^{[1]}(\xi, \hat{\omega}, t, \hat{\nu}) - (\hat{\omega} - 2\xi z t^2) \mathcal{I}^{[2]}(\xi, \hat{\omega}, t, \hat{\nu}) - \xi t \mathcal{I}^{[3]}(\xi, \hat{\omega}, t, \hat{\nu}) \right], \quad (23a)$$

$$\beta(\xi, \hat{\omega}, t, \hat{\nu}) = -\frac{\hat{\omega}^2 m_D^2}{2\mathcal{W}(\hat{\omega}, \hat{\nu})} \left[f_0(\xi) - z \mathcal{I}^{[0]}(\xi, \hat{\omega}, t, \hat{\nu}) - \xi t \mathcal{I}^{[1]}(\xi, \hat{\omega}, t, \hat{\nu}) \right], \quad (23b)$$

$$\gamma(\xi, \hat{\omega}, t, \hat{\nu}) = \frac{m_D^2}{2(1-t^2)} \left[\xi(1+t^2) f_1(\xi) - \hat{\omega} z(1+t^2) f_0(\xi) - \hat{\omega} \{ (1-t^2) - z^2(1+t^2) \} \mathcal{I}^{[0]}(\xi, \hat{\omega}, t, \hat{\nu}), \right. \\ \left. - t \{ 4\hat{\omega} z - 2\xi z^2 + \xi(1-t^2)(1+\hat{\omega} z) \} \mathcal{I}^{[1]}(\xi, \hat{\omega}, t, \hat{\nu}) \right. \\ \left. - \{ 4\xi z - 2\hat{\omega} - \xi(1-t^2)(\hat{\omega} + 3z) \} \mathcal{I}^{[2]}(\xi, \hat{\omega}, t, \hat{\nu}) + 2\xi t \mathcal{I}^{[3]}(\xi, \hat{\omega}, t, \hat{\nu}) \right], \quad (23c)$$

$$\delta(\xi, \hat{\omega}, t, \hat{\nu}) = \frac{\hat{\omega} m_D^2}{2(1-t^2)} \left[t z f_0(\xi) - t z^2 \mathcal{I}^{[0]}(\xi, \hat{\omega}, t, \hat{\nu}) + z(1-\xi t^2) \mathcal{I}^{[1]}(\xi, \hat{\omega}, t, \hat{\nu}) + \xi t \mathcal{I}^{[2]}(\xi, \hat{\omega}, t, \hat{\nu}) \right], \quad (23d)$$

$$\rho(\xi, \hat{\omega}, t, \hat{\nu}) = \frac{\hat{\omega} m_D^2}{2\mathcal{W}(\hat{\omega}, \hat{\nu})(1-t^2)} \left[\hat{\omega} t f_0(\xi) - \hat{\omega} t z \mathcal{I}^{[0]}(\xi, \hat{\omega}, t, \hat{\nu}) + \{ \hat{\omega}(1+\xi - \xi t^2) - \xi z \} \mathcal{I}^{[1]}(\xi, \hat{\omega}, t, \hat{\nu}) \right. \\ \left. + \xi t \mathcal{I}^{[2]}(\xi, \hat{\omega}, t, \hat{\nu}) \right], \quad (23e)$$

where $z = \hat{\omega} + i\hat{\nu}$. The master integral, $\mathcal{I}^{[n]}(\xi, \hat{\omega}, t, \hat{\nu})$ has the form

$$\mathcal{I}^{[n]}(\xi, \hat{\omega}, t, \hat{\nu}) = \int_{-1}^1 dy \frac{y^n}{(1+\xi y^2)^2} \int_0^{2\pi} d\phi \frac{1}{2\pi \hat{\omega} - \hat{\mathbf{p}} \cdot \mathbf{v} + i\hat{\nu}} \\ = \int_{-1}^1 dy \frac{y^n}{(1+\xi y^2)^2} \frac{\text{sign}(\text{Re}[\hat{\omega}] - \hat{p}_z y)}{\sqrt{(\hat{\omega} - \hat{p}_z y + i\hat{\nu})^2 - \hat{p}_y^2(1-y^2)}}, \\ = \int_{-1}^1 dy \frac{y^n}{(1+\xi y^2)^2} \frac{\text{sign}(\text{Re}[\hat{\omega}] - ty)}{\sqrt{(\hat{\omega} - ty + i\hat{\nu})^2 - (1-t^2)(1-y^2)}}, \quad (24)$$

where $n = 0, 1, 2, 3$ and $t = \cos \theta$, with θ being the angle between \mathbf{p} and \mathbf{n} . It is assumed that \mathbf{p} lies in the y - z plane, while \mathbf{n} is parallel to the z -axis. The ω generally has a complex value, and the integration variable y represents the cosine of the polar angle between \mathbf{k} and \mathbf{n} . The functions $f_0(\xi)$ and $f_1(\xi)$ are defined as

$$f_0(\xi) = \int_0^1 \frac{2}{(1+\xi y^2)^2} dy = \frac{1}{1+\xi} + \frac{\arctan \sqrt{\xi}}{\sqrt{\xi}}, \quad (25a)$$

$$f_1(\xi) = \int_0^1 \frac{2y^2}{(1+\xi y^2)^2} dy = -\frac{1}{\xi + \xi^2} + \frac{\arctan \sqrt{\xi}}{\sqrt{\xi^3}}. \quad (25b)$$

Note that, in the collisionless limit, that is, when the collision parameter $\nu = 0$, $\mathcal{W}(\hat{\omega}, 0) = 1$ and $z = \hat{\omega}$ only. Then,

$$\rho(\xi, \hat{\omega}, t, 0) = \delta(\xi, \hat{\omega}, t, 0), \quad (26)$$

The above relation implies that in the collisionless limit, we have only four structure functions, and the self-energy is symmetric, i.e., $\Pi^{ij} = \Pi^{ji}$.

As the dielectric permittivity of the medium is defined in the static limit ($\omega \rightarrow 0$), we can define various mass scales corresponding to the structure functions as

$$m_\alpha^2 = \lim_{\omega \rightarrow 0} \alpha, \quad (27a)$$

$$m_\beta^2 = -\lim_{\omega \rightarrow 0} \frac{\beta}{\hat{\omega}^2}, \quad (27b)$$

$$m_\gamma^2 = \lim_{\omega \rightarrow 0} \gamma, \quad (27c)$$

$$m_\delta^2 = \lim_{\omega \rightarrow 0} \frac{\tilde{n}}{\hat{\omega}} \text{Im}[\delta], \quad (27d)$$

$$m_\rho^2 = \lim_{\omega \rightarrow 0} \frac{\tilde{n}}{\hat{\omega}} \text{Im}[\rho]. \quad (27e)$$

After taking the static limit, the master integral $\mathcal{I}^{[n]}(\xi, 0, t, \hat{\nu})$, reduces to

$$\tilde{\mathcal{I}}^{[n]}(\xi, t, \hat{\nu}) = - \int_0^1 dy \frac{2}{(1 + \xi y^2)^2} f^{[n]}(y, t, \hat{\nu})$$

with

$$f^{[n]}(y, t, \hat{\nu}) = \begin{cases} \frac{\sqrt{s(y, t, \hat{\nu}) + y^2 - \hat{\nu}^2 + t^2 - 1}}{\sqrt{2s(y, t, \hat{\nu})}} y^n, & n \text{ is odd} \\ i \frac{\sqrt{2\hat{\nu}t/s(y, t, \hat{\nu})}}{\sqrt{s(y, t, \hat{\nu}) + y^2 - \hat{\nu}^2 + t^2 - 1}} y^{n+1}, & n \text{ is even} \end{cases}, \quad (28)$$

where $s(y, t, \hat{\nu}) \equiv \sqrt{(y^2 - \hat{\nu}^2 + t^2 - 1)^2 + 4y^2\hat{\nu}^2t^2}$. So the mass scales become [29]

$$m_\alpha^2 = -\frac{\xi t m_D^2}{2(1-t^2)} \left[t f_1(\xi) - (1-t^2 + \hat{\nu}^2) \tilde{\mathcal{I}}^{[1]}(\xi, t, \nu) - 2i\hat{\nu}t \tilde{\mathcal{I}}^{[2]}(\xi, t, \hat{\nu}) + \tilde{\mathcal{I}}^{[3]}(\xi, t, \hat{\nu}) \right], \quad (29a)$$

$$m_\beta^2 = \frac{m_D^2}{2\mathcal{W}(0, \hat{\nu})} \left[f_0(\xi) - i\hat{\nu} \tilde{\mathcal{I}}^{[0]}(\xi, t, \hat{\nu}) - \xi t \tilde{\mathcal{I}}^{[1]}(\xi, t, \hat{\nu}) \right], \quad (29b)$$

$$m_\gamma^2 = \frac{\xi m_D^2}{2(1-t^2)} \left[(1+t^2) f_1(\xi) - t(1-t^2 + 2\hat{\nu}^2) \tilde{\mathcal{I}}^{[1]}(\xi, t, \hat{\nu}) - i\hat{\nu}(1+3t^2) \tilde{\mathcal{I}}^{[2]}(\xi, t, \hat{\nu}) + 2t \tilde{\mathcal{I}}^{[3]}(\xi, t, \hat{\nu}) \right], \quad (29c)$$

$$m_\delta^2 = \frac{m_D^2}{2\sqrt{1-t^2}} \left[\hat{\nu} t f_0(\xi) - i\hat{\nu}^2 t \tilde{\mathcal{I}}^{[0]}(\xi, t, \hat{\nu}) + \hat{\nu}(1-\xi t^2) \tilde{\mathcal{I}}^{[1]}(\xi, t, \hat{\nu}) - i\xi t \tilde{\mathcal{I}}^{[2]}(\xi, t, \hat{\nu}) \right], \quad (29d)$$

$$m_\rho^2 = -\frac{m_D^2}{2\mathcal{W}(0, \hat{\nu})\sqrt{1-t^2}} \left[\xi \hat{\nu} \tilde{\mathcal{I}}^{[1]}(\xi, t, \hat{\nu}) + i\xi t \tilde{\mathcal{I}}^{[2]}(\xi, t, \hat{\nu}) \right], \quad (29e)$$

where the factor $\mathcal{W}(0, \hat{\nu}) = (1 - \hat{\nu} \operatorname{arccot} \hat{\nu})$ is real-valued, and hence, all mass scales are real-valued. It is worth mentioning that the master integrals can be evaluated analytically in the collision-less limit, and the mass scales at $\nu = 0$ become

$$m_{\alpha,0}^2 = -\frac{m_D^2 t^2}{2(1-t^2)} \left[f_0(\xi) - \frac{1}{1+\xi(1-t^2)} f_0\left(\frac{\xi t^2}{1+\xi(1-t^2)}\right) \right], \quad (30a)$$

$$m_{\beta,0}^2 = \frac{m_D^2}{2} \left[f_0(\xi) + \frac{\xi t^2}{(1+\xi(1-t^2))^2} f_0\left(\frac{\xi t^2}{1+\xi(1-t^2)}\right) \right], \quad (30b)$$

$$m_{\gamma,0}^2 = -\frac{m_D^2}{2(1-t^2)} \left[\frac{2(1-t^2)}{1+\xi} - (1+t^2) f_0(\xi) + \left(3 - \frac{1}{1+\xi(1-t^2)}\right) \frac{t^2}{1+\xi(1-t^2)} f_0\left(\frac{\xi t^2}{1+\xi(1-t^2)}\right) \right], \quad (30c)$$

$$m_{\delta,0}^2 = m_{\rho,0}^2 = -\frac{\pi}{4} \frac{m_D^2 \xi t \sqrt{1-t^2}}{[1+\xi(1-t^2)]^{3/2}}. \quad (30d)$$

III. DIELECTRIC PERMITTIVITY

In this section, we deduce the color dielectric permittivity in a collisional anisotropic QGP medium, which is later used to determine the in-medium heavy quarkonium potential. In the temporal axial gauge, this permittivity can be computed from the gluon propagator in the static limit as [27]

$$\epsilon^{-1}(p) = - \lim_{\omega \rightarrow 0} \omega^2 \frac{p^i p^j}{p^2} \Delta_{ij}(\omega, p) = \lim_{\omega \rightarrow 0} \omega^2 \frac{(p^2 - \omega^2 + \alpha + \gamma)}{(\omega^2 - \Omega_+^2)(\omega^2 - \Omega_-^2)}. \quad (31)$$

The dielectric permittivity depends on the gluon propagator, which has both the real and imaginary parts. Hence, it is a complex quantity with both real and imaginary parts, which can be written as

$$\operatorname{Re} \epsilon^{-1}(p) = - \lim_{\omega \rightarrow 0} \omega^2 \frac{p^i p^j}{p^2} \operatorname{Re} \Delta_{ij}(\omega, p). \quad (32)$$

In the static limit, the real part of the dielectric permittivity can be written in terms of the mass scales as

$$\begin{aligned}\text{Re } \epsilon^{-1}(p) &= \frac{p^2(p^2 + m_\alpha^2 + m_\gamma^2)}{\left(p^4 + p^2(m_\alpha^2 + m_\beta^2 + m_\gamma^2) + m_\alpha^2 m_\beta^2 + m_\beta^2 m_\gamma^2 - m_\delta^2 m_\rho^2\right)}, \\ &= \frac{p^2(p^2 + m_\alpha^2 + m_\gamma^2)}{(p^2 + m_+^2)(p^2 + m_-^2)},\end{aligned}\tag{33}$$

where

$$2m_\pm^2 = (m_\alpha^2 + m_\beta^2 + m_\gamma^2) \pm \sqrt{(m_\alpha^2 + m_\beta^2 + m_\gamma^2)^2 - 4\{m_\beta^2(m_\alpha^2 + m_\gamma^2) - m_\delta^2 m_\rho^2\}}.\tag{34}$$

Additionally, the imaginary part of the dielectric permittivity is given by

$$\text{Im } \epsilon^{-1}(p) = -\lim_{\omega \rightarrow 0} \omega^2 \frac{p^i p^j}{p^2} \text{Im} \Delta_{ij}(\omega, p).\tag{35}$$

Based on the spectral function approach [41], the imaginary part of the gluon propagator can be expressed as

$$\text{Im} \Delta^{ij} = -\pi(1 + e^{-\beta\omega}) \sum_m \mathbb{R}_m \mathcal{P}_m^{ij},\tag{36}$$

where $\mathcal{P}_m^{ij} = A^{ij}, B^{ij}, C^{ij}, D^{ij}, E^{ij}$ - are the projection operators and

$$\mathbb{R}_m = \frac{1}{\pi} \frac{e^{\beta\omega}}{e^{\beta\omega} - 1} \rho_m(\omega, p),\tag{37}$$

where

$$\rho_m(\omega, p) = \lim_{\omega \rightarrow 0} \text{Im}[(p^2 - \omega^2 + \alpha + \gamma)\Delta_G].\tag{38}$$

In the static limit ($\omega \rightarrow 0$), the imaginary part of the dielectric permittivity given in Eq. (35)) reduces to

$$\begin{aligned}\text{Im } \epsilon^{-1} &= -\lim_{\omega \rightarrow 0} \frac{e^{\beta\omega} + 1}{e^{\beta\omega} - 1} \omega^2 \text{Im} \left(\frac{p^2 - \omega^2 + \alpha + \gamma}{(\omega^2 - \Omega_+^2)(\omega^2 - \Omega_-^2)} \right) \\ &\approx \lim_{\omega \rightarrow 0} \frac{2\omega T}{(\Re\Omega_+^2)^2} \frac{1}{(\omega^2 - \Re\Omega_-^2)^2} \left[(p^2 + m_\alpha^2 + m_\gamma^2) \{ \Re\Omega_+^2 \Im\Omega_-^2 - \Im\Omega_+^2 (\omega^2 - \Re\Omega_-^2) \} \right. \\ &\quad \left. + (\Im\alpha + \Im\gamma) \Re\Omega_+^2 (\omega^2 - \Re\Omega_-^2) \right] \\ &= \lim_{\omega \rightarrow 0} \frac{2T}{(\Re\Omega_+^2)^2} \frac{1}{\left(1 - \frac{\Re\Omega_-^2}{\omega^2}\right)^2} \left[(p^2 + m_\alpha^2 + m_\gamma^2) \left\{ \Re\Omega_+^2 \frac{\Im\Omega_-^2}{\omega^3} - \frac{\Im\Omega_+^2}{\omega} \left(1 - \frac{\Re\Omega_-^2}{\omega^2}\right) \right\} \right. \\ &\quad \left. + \left(\frac{\Im\alpha}{\omega} + \frac{\Im\gamma}{\omega}\right) \Re\Omega_+^2 \left(1 - \frac{\Re\Omega_-^2}{\omega^2}\right) \right].\end{aligned}\tag{39}$$

To determine $\text{Im}\epsilon^{-1}$, we need to evaluate the following quantities in the static limit as

$$\begin{aligned}\lim_{\omega \rightarrow 0} \Re\Omega_+^2 &\approx (p^2 + m_\alpha^2 + m_\gamma^2) + \mathcal{O}(\omega), \\ \lim_{\omega \rightarrow 0} \Re\Omega_-^2 &\approx \frac{\omega^2}{p^2} \left[-m_\beta^2 + \frac{2m_\rho^2 m_\delta^2}{p^2 + m_\alpha^2 + m_\gamma^2} \right] + \mathcal{O}(\omega^3), \\ \lim_{\omega \rightarrow 0} \Im\Omega_+^2 &\approx (\Im\alpha + \Im\gamma) + \mathcal{O}(\omega^2), \\ \lim_{\omega \rightarrow 0} \Im\Omega_-^2 &\approx \Im\beta + \mathcal{O}(\omega^4).\end{aligned}\tag{40}$$

Using the static limit from Eq. (40) in Eq. (39), we get

$$\begin{aligned}
\text{Im } \epsilon^{-1}(p, \xi, \nu, t) &= \lim_{\omega \rightarrow 0} \frac{2\Im\beta p^4 T (p^2 + m_\alpha^2 + m_\gamma^2)^2}{\omega^3 \left(p^4 + p^2 (m_\alpha^2 + m_\beta^2 + m_\gamma^2) + m_\alpha^2 m_\beta^2 + m_\beta^2 m_\gamma^2 - m_\delta^2 m_\rho^2 \right)^2} \\
&= - \frac{\pi m_{i\beta}^2 p T (p^2 + m_\alpha^2 + m_\gamma^2)^2}{\left(p^4 + p^2 (m_\alpha^2 + m_\beta^2 + m_\gamma^2) + m_\alpha^2 m_\beta^2 + m_\beta^2 m_\gamma^2 - m_\delta^2 m_\rho^2 \right)^2}, \\
&= - \frac{\pi m_{i\beta}^2 p T (p^2 + m_\alpha^2 + m_\gamma^2)^2}{(p^2 + m_+^2)^2 (p^2 + m_-^2)^2}.
\end{aligned} \tag{41}$$

In Eq. (41), we introduce a new mass scale $m_{i\beta}$ as

$$\begin{aligned}
m_{i\beta}^2 &= -\frac{2}{\pi} \lim_{\omega \rightarrow 0} \frac{p^3}{\omega^3} \Im\beta \\
&= \frac{2}{\pi \mathcal{W}(0, \hat{\nu})} \left[\frac{\hat{\nu}}{1 + \hat{\nu}^2} m_\beta^2 - \frac{m_D^2}{2} \left\{ \tilde{\mathcal{J}}(\xi, t, \hat{\nu}) - i \tilde{\mathcal{I}}^{[0]}(\xi, t, \hat{\nu}) \right\} \right],
\end{aligned} \tag{42}$$

where

$$\tilde{\mathcal{J}}(\xi, t, \hat{\nu}) = \int_{-1}^1 \frac{(\hat{\nu} + itx)(i\hat{\nu} + \xi tx) \text{sgn}(tx)}{(1 + \xi x^2)^2 [(tx - i\hat{\nu})^2 - (1 - t^2)(1 - x^2)]^{3/2}} dx. \tag{43}$$

In the collision-less medium ($\nu = 0$), the new mass scale $m_{i\beta}$ becomes

$$\begin{aligned}
m_{i\beta,0}^2 &= \lim_{\hat{\nu} \rightarrow 0} \frac{m_D^2}{\pi} \left[i \tilde{\mathcal{I}}^{[0]}(\xi, t, \hat{\nu}) - \tilde{\mathcal{J}}(\xi, t, \hat{\nu}) \right] \\
&= \frac{m_D^2}{(1 + (1 - t^2)\xi)^{3/2}} \left[1 + \frac{\xi(1 + t^2) + \xi(1 - t^2)(1 - 2t^2)}{1 + (1 - t^2)\xi} \right].
\end{aligned} \tag{44}$$

With the analytic form of mass scales in Eq. (30) and (44), one can express the $\text{Im}\epsilon^{-1}(\nu = 0)$ in the analytic form using Eq. (41). In the earlier literature, the analytic form of $\text{Im}\epsilon^{-1}(\nu = 0)$ was never obtained for a collisionless anisotropic medium, in our knowledge.

Lastly, in the limit $\xi = \nu = 0$, all the mass scales becomes

$$\begin{aligned}
m_\alpha^2 &= m_\gamma^2 = m_\delta^2 = m_\rho^2 = m_-^2 = 0, \\
m_\beta^2 &= m_{i\beta}^2 = m_+^2 = m_D^2.
\end{aligned} \tag{45}$$

The dielectric permittivity will be used to compute the in-medium heavy quark-antiquark potential.

IV. IN-MEDIUM HEAVY QUARK-ANTIQUARK POTENTIAL

In this section, we investigate the effect of a collisional anisotropic medium on the in-medium heavy quark potential. We compute the in-medium heavy quark-antiquark potential by correcting the Cornell potential in momentum space using the dielectric permittivity (31), which accounts for the effects of the collisional anisotropic thermal medium [17, 33, 36]

$$V(\mathbf{r}, \xi, \nu, T) = \int \frac{d^3\mathbf{p}}{(2\pi)^{3/2}} (e^{i\mathbf{p}\cdot\mathbf{r}} - 1) \frac{V_C(p)}{\epsilon(p, \xi, \nu)}, \tag{46}$$

where $V_C(p) = -\sqrt{(2/\pi)}(\alpha/p^2 + 2\sigma/p^4)$ [17] is the Fourier transform of the vacuum Cornell potential $V_C(r) = -\alpha/r + \sigma r$. Here $\alpha = C_F \alpha_s$ with $C_F = 4/3$ being the Casimir fundamental and α_s being the strong coupling constant

$$\alpha_s(\Lambda^2) = \frac{12\pi}{(11N_c - 2N_f) \ln\left(\frac{\Lambda^2}{\Lambda_{\text{MS}}^2}\right)}, \tag{47}$$

In Eq. (47), $N_c = 3$ and $\Lambda_{\overline{\text{MS}}} = 0.176$ GeV for $N_f = 3$ and $\Lambda = 2\pi T$. Here the string tension, σ , is taken as $(0.44)^2$ GeV². After substituting Eq. 31 into Eq. 46, we obtain the medium-modified complex heavy-quark potential in an anisotropic medium, whose real part reads

$$\begin{aligned} \text{Re } V(r, \xi, \nu, T) &= \int \frac{d^3\mathbf{p}}{(2\pi)^{3/2}} (e^{i\mathbf{p}\cdot\mathbf{r}} - 1) V_C(p) \text{Re } \epsilon^{-1}(p, \xi, \nu) \\ &= -\frac{1}{2\pi^2} \int d^3\mathbf{p} (e^{i\mathbf{p}\cdot\mathbf{r}} - 1) \frac{(p^2 + m_\alpha^2 + m_\gamma^2)}{(p^2 + m_+^2)(p^2 + m_-^2)} \left(\alpha + \frac{2\sigma}{p^2} \right). \end{aligned} \quad (48)$$

For general direction of \mathbf{r} with the anisotropy direction, $\hat{\mathbf{n}}$, we will have, $\mathbf{p}\cdot\mathbf{r} = rp[\sin\theta \sin\Theta \cos(\phi - \Phi) + \cos\theta \cos\Theta]$, where $\theta(\Theta)$ and $\phi(\Phi)$ are the polar and the azimuthal angles in momentum (coordinate) space with the anisotropy direction, respectively, since we take $\hat{\mathbf{n}} = \hat{\mathbf{z}}$. After an integration over the azimuthal angle of the $(\exp(i\mathbf{p}\cdot\mathbf{r}) - 1)$, Eq. (48) becomes

$$\begin{aligned} \Re V(r, \xi, \nu, T) &= -\frac{1}{\pi} \int_{p=0}^{\infty} \int_{\theta=0}^{\pi} p^2 dp \sin\theta d\theta [e^{ipr \cos\theta \cos\Theta} J_0(pr \sin\theta \sin\Theta) - 1] \\ &\quad \times \frac{(p^2 + m_\alpha^2 + m_\gamma^2)}{(p^2 + m_+^2)(p^2 + m_-^2)} \left(\alpha + \frac{2\sigma}{p^2} \right), \\ &= -\frac{2}{\pi} \int_{p=0}^{\infty} \int_{t=0}^1 p^2 dp dt [e^{ipr t \cos\Theta} J_0(pr \sqrt{1-t^2} \sin\Theta) - 1] \\ &\quad \times \frac{(p^2 + m_\alpha^2 + m_\gamma^2)}{(p^2 + m_+^2)(p^2 + m_-^2)} \left(\alpha + \frac{2\sigma}{p^2} \right), \end{aligned} \quad (49)$$

where J_0 is the Bessel's function of the first kind. Now, in the Coulomb part of the potential, Eq. (49) has a zero-temperature UV divergence, and that is set to zero, giving us

$$\begin{aligned} \Re V(r, \xi, \nu, T) &= -\frac{2}{\pi} \int_{p=0}^{\infty} \int_{t=0}^1 p^2 dp dt [e^{ipr t \cos\Theta} J_0(pr \sqrt{1-t^2} \sin\Theta) - 1] \\ &\quad \times \frac{(p^2 + m_\alpha^2 + m_\gamma^2)}{(p^2 + m_+^2)(p^2 + m_-^2)} \left(\alpha + \frac{2\sigma}{p^2} \right) - \frac{2}{\pi} \int_{p=0}^{\infty} dp \alpha. \end{aligned} \quad (50)$$

Note that for a collisionless, isotropy plasma, the real part of the quarkonium potential is

$$\Re V_{\text{HTL}}(r, T) = -\alpha m_D \left(1 + \frac{e^{-m_D r}}{m_D r} \right) + \frac{2\sigma}{m_D} \left(1 + \frac{e^{-m_D r} - 1}{m_D r} \right). \quad (51)$$

In Fig. 1, we plot the real part of the potential (Eq. (49)) as a function of the separation distance (r) at temperature $T = 0.2$ GeV. The left panel illustrates the results for various values of the collision parameter, ν , and anisotropy parameter, ξ when the $Q\bar{Q}$ dipole axis is aligned parallel to the anisotropy axis, while the right panel shows the results when the dipole is aligned transverse to the anisotropy axis. Here, the solid black line shows the real part of the potential for the isotropic collisionless plasma (Eq. (51)) when $\xi = 0$ and $\nu = 0$, while various colors denote the various values of the collision parameter, ν . We find that the real part of the potential has nominal effects with increasing collisional parameter ν . Notably, the impact of ν on the real part of the potential remains nearly consistent for both parallel and transverse alignments.

The imaginary part of the potential is written as

$$\begin{aligned} \text{Im } V(r, \xi, \nu, T) &= \int \frac{d^3\mathbf{p}}{(2\pi)^{3/2}} (e^{i\mathbf{p}\cdot\mathbf{r}} - 1) V_C(p) \text{Im } \epsilon^{-1}(p, \xi, \nu) \\ &= -\frac{1}{\pi} \int_{p=0}^{\infty} \int_{\theta=0}^{\pi} p^2 dp \sin\theta d\theta [e^{ipr \cos\theta \cos\Theta} J_0(pr \sin\theta \sin\Theta) - 1] \\ &\quad \times \frac{1}{p^2} \left(\alpha + \frac{2\sigma}{p^2} \right) \frac{-\pi m_{i\beta}^2 p T (p^2 + m_\alpha^2 + m_\gamma^2)^2}{(p^2 + m_+^2)^2 (p^2 + m_-^2)^2} \\ &= -\frac{1}{\pi} \int_{p=0}^{\infty} \int_{t=0}^1 p^2 dp dt [\cos(pr t \cos\Theta) J_0(pr \sqrt{1-t^2} \sin\Theta) - 1] \\ &\quad \times \frac{2}{p^2} \left(\alpha + \frac{2\sigma}{p^2} \right) \frac{-\pi m_{i\beta}^2 p T (p^2 + m_\alpha^2 + m_\gamma^2)^2}{(p^2 + m_+^2)^2 (p^2 + m_-^2)^2}, \end{aligned} \quad (52)$$

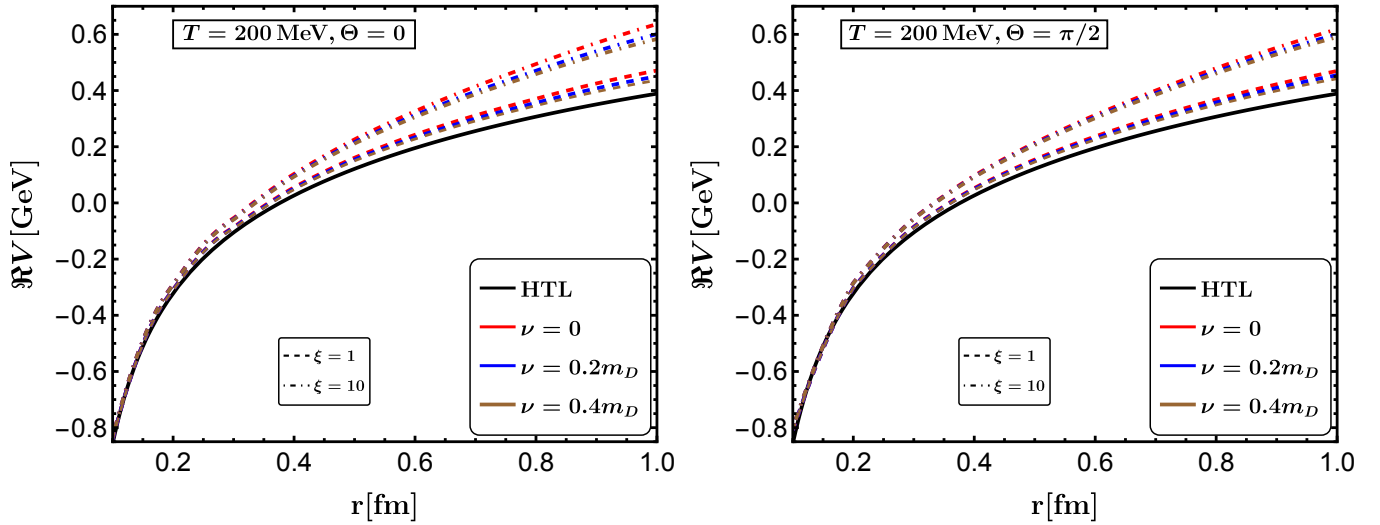


FIG. 1: The real part of the potential as a function of separation distance r for various values of ν and ξ when $Q\bar{Q}$ is aligned parallel ($\Theta = 0$) (left) and aligned transverse ($\Theta = \pi/2$) (right) to the direction of anisotropy at $T = 0.2$ GeV. In both the figures, the dashed lines represent $\xi = 1$ case, whereas dot-dashed lines represent $\xi = 10$ case.

where $t = \cos\theta$. Note that for the isotropy case in the absence of the collisional term, the imaginary potential reduces to

$$\text{Im } V_{\text{HTL}}(r, T) = -2Tm_D^2 \int \frac{p dp}{(p^2 + m_D^2)^2} \left(\alpha + \frac{2\sigma}{p^2} \right) \left(1 - \frac{\sin pr}{pr} \right). \quad (53)$$

In Fig. 2, we plot the imaginary part of the potential (52) as a function of separation distance r at temperature

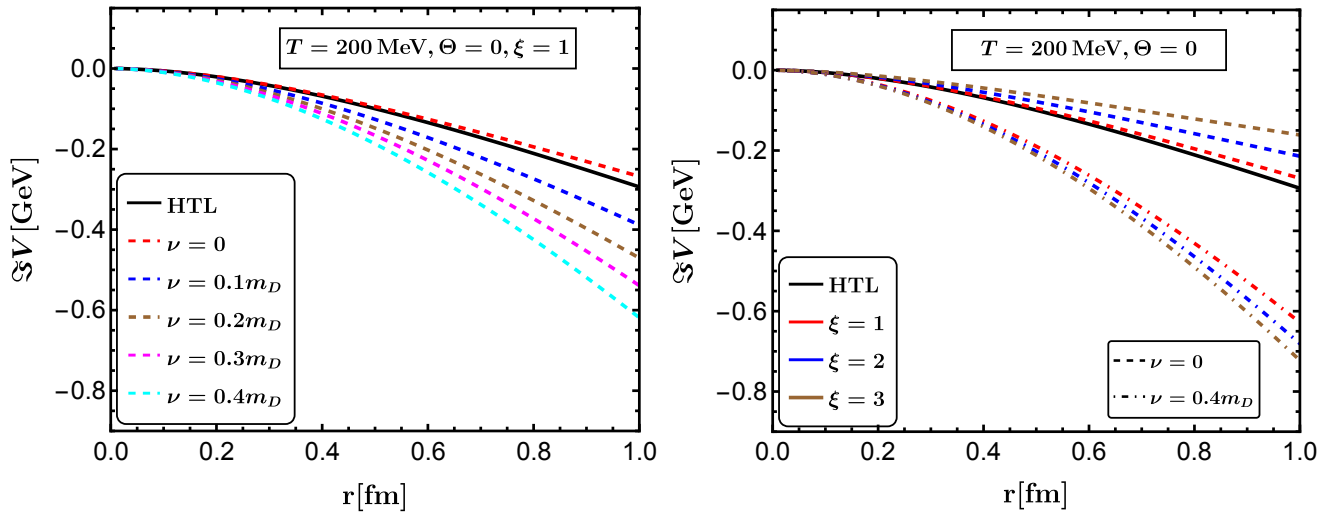


FIG. 2: The imaginary part of the potential as a function of separation distance r for different values of ν (left) and ξ (right) at $T = 0.2$ GeV and $\Theta = 0$.

$T = 0.2$ GeV when the dipole axis $Q\bar{Q}$ is aligned parallel to the direction of anisotropy. The left panel shows the results for various values of ν while keeping $\xi = 1$. We find that the imaginary part of the potential increases in magnitude as ν increases. The right panel presents the results for the different values of ξ . The dashed and dash-dotted lines correspond to $\nu = 0$ and $\nu = 0.4m_D$, respectively. In this case, we observe that the imaginary part of the potential is suppressed at larger r with the increase in the anisotropic parameter ξ for $\nu = 0$, consistent with previous findings

in the literature. However, for $\nu = 0.4m_D$, the imaginary part of the potential shows the opposite behavior as it increases in magnitude with the increase in ξ . The solid black line shows the imaginary part of the potential for the isotropic collisionless plasma (53).

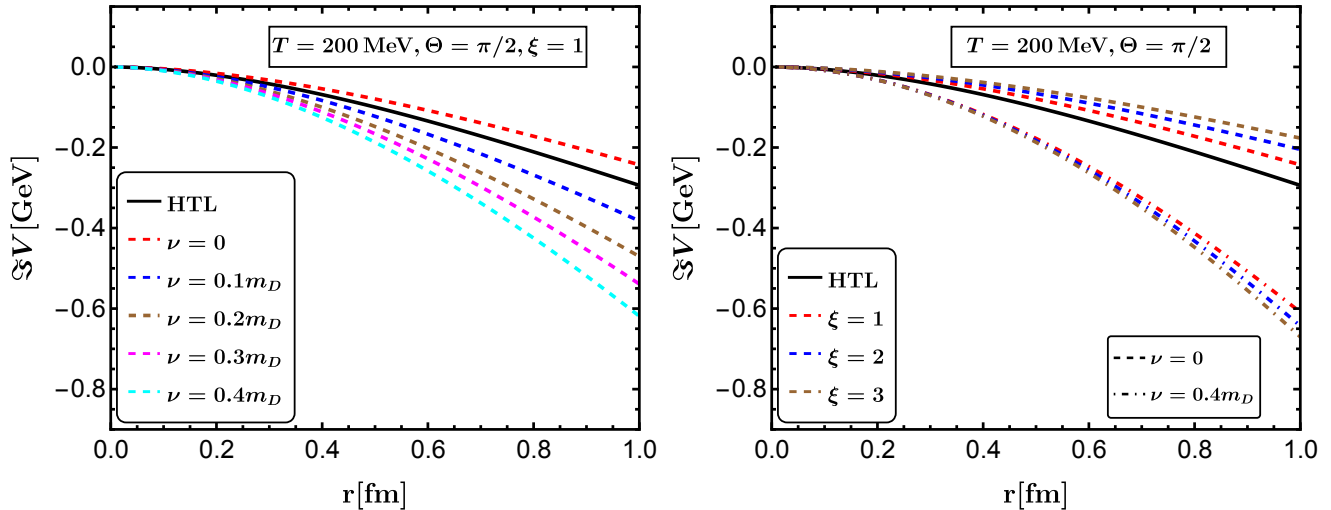


FIG. 3: The imaginary part of the potential as a function of r for different values of ν (left) and ξ (right) at $T = 0.2$ GeV and $\Theta = \pi/2$.

Fig. 3 shows a similar plot of the imaginary part of the potential for the perpendicular orientation of the $Q\bar{Q}$ dipole axis relative to the direction of anisotropy. The effect of ν on the imaginary part of the potential is similar for both the parallel and perpendicular orientations. Notably, the impact of ν is more pronounced on the imaginary part of the potential compared to the real part, where its effect is minimal.

V. DECAY WIDTH

In this section, we determine the decay width of quarkonium states based on the imaginary part of the potential obtained earlier. Treating this imaginary component as a perturbation to the vacuum potential allows us to estimate the thermal width, Γ , of the quarkonium states as

$$\begin{aligned}
\Gamma(\xi, \nu, T) &= - \int_{\mathbf{r}} |\psi(\mathbf{r}, T)|^2 \text{Im}V(\mathbf{r}, \xi, \nu, T) \\
&= -2\pi \int_{r=0}^{\infty} dr r^2 \int_{\Theta=0}^{\pi} d\Theta \sin(\Theta) |\psi(r, T)|^2 \text{Im}V(r, \Theta, \xi, \nu, T) \\
&= -\frac{2}{a_0^3} \int_{r=0}^{\infty} dr r^2 \int_{\Theta=0}^{\pi} d\Theta \sin(\Theta) e^{-2r/a_0(T)} \text{Im}V(r, \Theta, \xi, \nu, T) \\
&= \frac{4}{\pi a_0^3} \int_{r=0}^{\infty} dr r^2 \int_{\Theta=0}^{\pi} d\Theta \sin(\Theta) e^{-2r/a_0(T)} \int_{p=0}^{\infty} \int_{t=0}^1 dp dt \\
&\quad \times \left[\cos(pr t \cos \Theta) J_0(pr \sqrt{1-t^2} \sin \Theta) - 1 \right] \left(\alpha + \frac{2\sigma}{p^2} \right) \text{Im}\epsilon^{-1}(p, \xi, \nu, T), \tag{54}
\end{aligned}$$

where we have used the Coulombic ground state wave function

$$\psi(r, T) = \frac{1}{\sqrt{\pi a_0(T)^3}} e^{-r/a_0(T)}, \quad \text{and} \quad a_0(T) = \frac{2}{m_0 \alpha(T)} \tag{55}$$

is the Bohr radius of the heavy quarkonium system, and the charmonium (J/ψ) mass is taken as $m_0 = 1.275$ GeV. The primary contribution to the imaginary potential for a deeply bound state involving heavy quarks is Coulombic in nature. This supports the use of Coulomb wave functions for calculating the decay width.

The r -integration in Eq. (54) can be computed using the integral

$$\int_0^\infty r^2 e^{-ar} J_0(cr) dr = \frac{2a^2 - c^2}{(a^2 + c^2)^{5/2}}. \quad (56)$$

The integral relation in Eq. (56) can be used for the following integration as

$$\int_0^\infty r^2 e^{-ar} \cos(br) J_0(cr) dr = \frac{1}{2} \left[\frac{2(a+ib)^2 - c^2}{((a+ib)^2 + c^2)^{5/2}} + \frac{2(a-ib)^2 - c^2}{((a-ib)^2 + c^2)^{5/2}} \right]. \quad (57)$$

In Eq. (54),

$$a = \frac{2}{a_0}, \quad (58a)$$

$$b = pr t \cos \Theta, \quad (58b)$$

$$c = pr \sqrt{1-t^2} \sin \Theta. \quad (58c)$$

So, Eq. (54) becomes

$$\begin{aligned} \Gamma(T, \xi, \nu) &= \int_{p=0}^\infty \int_{t=0}^1 \int_{\Theta=0}^\pi \frac{4 \sin \Theta}{\pi a_0^3} \left[\frac{\left(\frac{2}{a_0} - ipt \cos \Theta\right)^2 - \frac{1}{2} p^2 (1-t^2) \sin^2 \Theta}{\left(\frac{2}{a_0} - ipt \cos \Theta\right)^2 + p^2 (1-t^2) \sin^2 \Theta} \right. \\ &\quad \left. + \frac{\left(\frac{2}{a_0} + ipt \cos \Theta\right)^2 - \frac{1}{2} p^2 (1-t^2) \sin^2 \Theta}{\left(\frac{2}{a_0} + ipt \cos \Theta\right)^2 + p^2 (1-t^2) \sin^2 \Theta} - \frac{a_0^3}{4} \right] \left(\alpha + \frac{2\sigma}{p^2} \right) \text{Im} \epsilon^{-1} dp dt d\Theta \\ &= \frac{2}{\pi} \int_{p=0}^\infty \int_{t=0}^1 \left[\frac{16}{(a_0^2 p^2 + 4)^2} - 1 \right] \left(\alpha + \frac{2\sigma}{p^2} \right) \text{Im} \epsilon^{-1}(p, \xi, \nu, t) dp dt. \end{aligned} \quad (59)$$

For an isotropic, collisionless medium, the decay width of quarkonium can be obtained analytically as

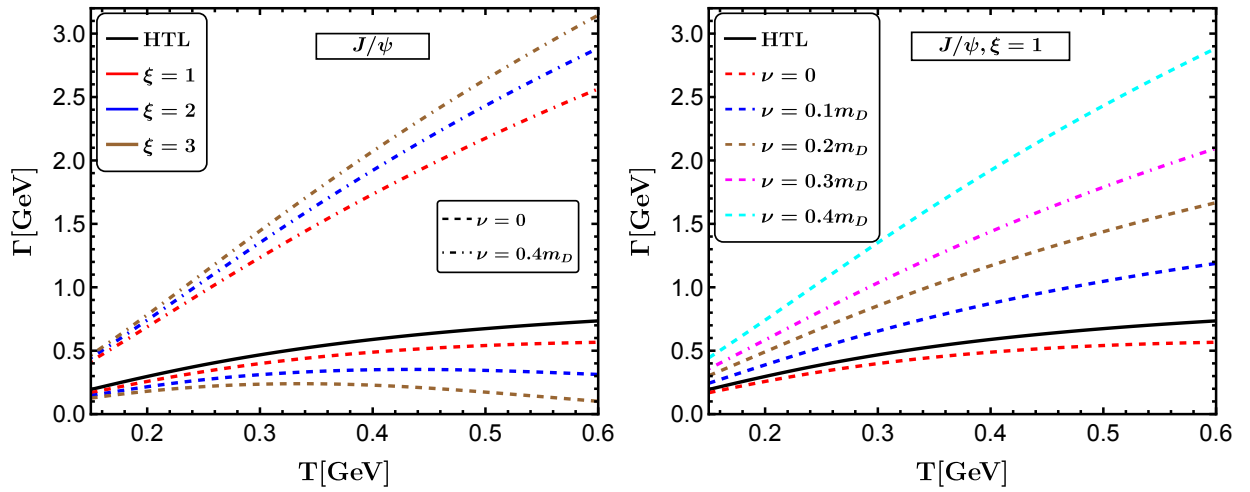


FIG. 4: Temperature variation of decay width for the ground state of charmonium.

$$\begin{aligned}
\Gamma_{\text{HTL}} &= \frac{2}{\pi} \int_{p=0}^{\infty} \int_{t=0}^1 \left[\frac{16}{(a_0^2 p^2 + 4)^2} - 1 \right] \left(\alpha + \frac{2\sigma}{p^2} \right) \frac{-\pi T p m_D^2}{(p^2 + m_D^2)^2} dp dt \\
&= \frac{\alpha m_D^2 a_0^2 T}{(a_0^2 m_D^2 - 4)} \left[1 - \frac{8}{(a_0^2 m_D^2 - 4)} + \frac{64}{(a_0^2 m_D^2 - 4)^2} \log \frac{m_D a_0}{2} \right] \\
&\quad + \frac{4\sigma a_0^2 T}{(a_0^2 m_D^2 - 4)^2} \left[4 + \frac{a_0^2 m_D^2 (a_0^2 m_D^2 - 12)}{(a_0^2 m_D^2 - 4)} \log \frac{m_D a_0}{2} \right]. \tag{60}
\end{aligned}$$

In Fig.(4), we plot the decay width of the ground state of charmonium (J/ψ) as a function of temperature T . The solid black line represents the decay width calculated for the isotropic, collisionless medium (eq. (60)). In the left panel, the dashed lines indicate the collisionless case ($\nu = 0$), while the dash-dotted lines correspond to the collisional case with $\nu = 0.4m_D$. The different colors represent various values of ξ . In the right panel, the different colored dash-dotted lines indicate various values of ν for $\xi = 1$. We observe that the decay width increases with both temperature and the collisional parameter. In the collisional case, the magnitude of the decay width is enhanced as ξ increases. This behavior is related to the characteristics of the imaginary part discussed in the previous section. The finding at $\nu = 0$ aligns with the decay width results obtained in the small anisotropy limit in Ref. [33].

VI. SUMMARY AND DISCUSSIONS

In this article, we studied the complex heavy quarkonium potential in a QGP medium in the presence of a momentum-space anisotropy, considering the effect of collisions among the plasma constituents. The anisotropic correction in momentum space is applied by considering the Romatschke-Strickland anisotropy distribution function of the thermal partons. Consequently, the gluon self-energy is rederived by solving linearized kinetic equations of the Boltzmann-Vlasov type, incorporating the BGK collision kernel. We further computed the resummed gluon propagator, based on which we calculated the real and imaginary parts of the dielectric permittivity of the medium in the static limit. Using this dielectric permittivity, we derived the complex potential for heavy quarkonia and analyzed how this potential is affected in the presence of a collisional anisotropic medium. We observed that the momentum-space anisotropic correction, parameterized by ξ , reduces the screening effect. The anisotropy in momentum space makes the potential anisotropic that depends on the angle Θ between the $Q\bar{Q}$ dipole axis and the direction of anisotropy. Though the momentum-space anisotropy reduces the screening, the effect of the collision in the real part of the potential is nominal. Additionally, the magnitude of the imaginary part of the potential is enhanced with the collisional parameter ν . The magnitude of the imaginary part of the potential is suppressed with ξ when $\nu = 0$, whereas it is enhanced for a non-zero value of ν . Further, we calculated the decay width of J/ψ . We found that the decay width decreases with the increase in anisotropy for a collisionless plasma. However, the decay width increases with the increase of anisotropy in the presence of the collision among the plasma constituents. So, the charmonium dissociates faster in a collisional plasma.

We look forward to using our complex potential to calculate the binding energy and dissociation temperature in the near future.

ACKNOWLEDGMENTS

L. T. would like to acknowledge the support of the National Research Foundation (NRF), funded by the Ministry of Science of Korea (Grant No. 2021R1F1A1061387).

Appendix A: Calculations of structure functions

We take anisotropy direction $\mathbf{n} = \hat{z}$ and assume \mathbf{k} lies in the (yz) plane, i.e., $\mathbf{k} = (0, k_y, k_z)$. In general, k_y should be replaced by k_\perp .

$$\begin{aligned}
\beta &= \hat{k}^i \hat{k}^j m_D^2 \int \frac{d\Omega}{4\pi} v^i \frac{v^l + \xi(\mathbf{v} \cdot \mathbf{n})n^l}{(1 + \xi(\mathbf{v} \cdot \mathbf{n})^2)^2} \frac{\delta^{lj}(\hat{\omega} - \hat{\mathbf{p}} \cdot \mathbf{v}) + \hat{p}^l v^j}{\hat{\omega} - \hat{\mathbf{p}} \cdot \mathbf{v} + i\hat{\nu}} \\
&+ \hat{k}^i \hat{k}^j m_D^2 (i\hat{\nu}) \int \frac{d\Omega'}{4\pi} \frac{v'^i}{\hat{\omega} - \hat{\mathbf{p}} \cdot \mathbf{v}' + i\hat{\nu}} \int \frac{d\Omega}{4\pi} \frac{v^l + \xi(\mathbf{v} \cdot \mathbf{n})n^l}{(1 + \xi(\mathbf{v} \cdot \mathbf{n})^2)^2} \frac{\delta^{lj}(\hat{\omega} - \hat{\mathbf{p}} \cdot \mathbf{v}) + \hat{p}^l v^j}{\hat{\omega} - \hat{\mathbf{p}} \cdot \mathbf{v} + i\hat{\nu}} \mathcal{W}(\hat{\omega}, \hat{\nu})^{-1} \\
&= m_D^2 \int \frac{d\Omega}{4\pi} (\hat{\mathbf{k}} \cdot \mathbf{v}) \frac{v^l + \xi \cos \theta n^l}{(1 + \xi \cos^2 \theta)^2} \frac{\hat{k}^l (\hat{\omega} - \hat{\mathbf{k}} \cdot \mathbf{v}) + \hat{k}^l (\hat{\mathbf{k}} \cdot \mathbf{v})}{\hat{\omega} - \hat{\mathbf{k}} \cdot \mathbf{v} + i\hat{\nu}} + m_D^2 \int \frac{d\Omega'}{4\pi} \frac{\hat{\mathbf{k}} \cdot \mathbf{v}'}{(\hat{\omega} - \hat{\mathbf{k}} \cdot \mathbf{v}' + i\hat{\nu})} \\
&\times \int \frac{d\Omega}{4\pi} \frac{v^l + \xi \cos \theta n^l}{(1 + \xi \cos^2 \theta)^2} \frac{\hat{k}^l (\hat{\omega} - \hat{\mathbf{k}} \cdot \mathbf{v}) + \hat{k}^l (\hat{\mathbf{k}} \cdot \mathbf{v})}{\hat{\omega} - \hat{\mathbf{k}} \cdot \mathbf{v} + i\hat{\nu}} \mathcal{W}(\hat{\omega}, \hat{\nu})^{-1} \\
&= m_D^2 \int \frac{d\Omega}{4\pi} \hat{\omega} \left(\frac{\hat{\omega} + i\hat{\nu}}{\hat{\omega} + i\hat{\nu} - \hat{\mathbf{k}} \cdot \mathbf{v}} - 1 \right) \frac{\hat{\mathbf{k}} \cdot \mathbf{v} + \xi t \cos \theta}{(1 + \xi \cos^2 \theta)^2} + (i\hat{\nu}) m_D^2 \int \frac{d\Omega'}{4\pi} \left(\frac{\hat{\omega} + i\hat{\nu}}{\hat{\omega} + i\hat{\nu} - \hat{\mathbf{k}} \cdot \mathbf{v}'} - 1 \right) \\
&\times \int \frac{d\Omega}{4\pi} \frac{\hat{\mathbf{k}} \cdot \mathbf{v} + \xi t \cos \theta}{(1 + \xi \cos^2 \theta)^2} \frac{\hat{\omega}}{\hat{\omega} + i\hat{\nu} - \hat{\mathbf{k}} \cdot \mathbf{v}} \mathcal{W}(\hat{\omega}, \hat{\nu})^{-1} \\
&= \beta_1 + \beta_2.
\end{aligned} \tag{A1}$$

Here,

$$\begin{aligned}
\beta_1 &= m_D^2 \int \frac{d\Omega}{4\pi} \hat{\omega} \left(\frac{\hat{\omega} + i\hat{\nu}}{\hat{\omega} + i\hat{\nu} - \hat{\mathbf{k}} \cdot \mathbf{v}} - 1 \right) \frac{\hat{\mathbf{k}} \cdot \mathbf{v} + \xi t \cos \theta}{(1 + \xi \cos^2 \theta)^2} \\
&= \hat{\omega} m_D^2 \left[\int_{-1}^1 \frac{dx}{2} \int_0^{2\pi} \frac{d\phi}{2\pi} \frac{1}{(1 + \xi x^2)^2} \frac{z(z + \xi t x)}{z - \hat{\mathbf{k}} \cdot \mathbf{v}} - \int_{-1}^1 \frac{dx}{2} \int_0^{2\pi} \frac{d\phi}{2\pi} \frac{z}{(1 + \xi x^2)^2} \right] \\
&= \hat{\omega} m_D^2 \left[\int_{-1}^1 \frac{dx}{2} \int_0^{2\pi} \left(\frac{z^2}{z - \hat{\mathbf{k}} \cdot \mathbf{v}} + z \xi t \frac{x}{z - \hat{\mathbf{k}} \cdot \mathbf{v}} \right) \frac{1}{(1 + \xi x^2)^2} - \frac{z}{2} f_0(\xi) \right],
\end{aligned} \tag{A2}$$

and

$$\begin{aligned}
\beta_2 &= i\hat{\nu} m_D^2 \int \frac{d\Omega'}{4\pi} \left(\frac{z}{z - \hat{\mathbf{k}} \cdot \mathbf{v}'} - 1 \right) \int \frac{d\Omega}{4\pi} \frac{\hat{\mathbf{k}} \cdot \mathbf{v} + \xi t \cos \theta}{(1 + \xi \cos^2 \theta)^2} \frac{\hat{\omega}}{\hat{\omega} + i\hat{\nu} - \hat{\mathbf{k}} \cdot \mathbf{v}} \mathcal{W}(\hat{\omega}, \hat{\nu})^{-1} \\
&= \frac{[z - z\mathcal{W}(\hat{\omega}, \hat{\nu}) - i\hat{\nu}]\hat{\omega}}{\mathcal{W}(\hat{\omega}, \hat{\nu})} \left[\frac{z}{2} \mathcal{I}^{[0]}(\xi, \hat{\omega}, t, \hat{\nu}) + \frac{\xi t}{2} \mathcal{I}^{[1]}(\xi, \hat{\omega}, t, \hat{\nu}) - \frac{f_0(\xi)}{2} \right].
\end{aligned} \tag{A3}$$

Combining the above two equations, we get,

$$\beta(\xi, \hat{\omega}, t, \hat{\nu}) = -\frac{\hat{\omega}^2 m_D^2}{2\mathcal{W}(\hat{\omega}, \hat{\nu})} [f_0(\xi) - z\mathcal{I}^{[0]}(\xi, \hat{\omega}, t, \hat{\nu}) - \xi t \mathcal{I}^{[1]}(\xi, \hat{\omega}, t, \hat{\nu})]. \tag{A4}$$

Now, From Eq. (16), we can obtain,

$$\alpha = \text{Tr} \Pi^{ij} - \frac{1}{\tilde{n}^2} \tilde{n}^i \Pi^{ij} \tilde{n}^j - \beta, \tag{A5}$$

with

$$\begin{aligned}
\text{Tr} \Pi^{ij} &= \Pi^{ii} \\
&= \frac{m_D^2}{2} \left[\xi f_1(\xi) + \hat{\omega} \mathcal{I}^{[0]}(\xi, \hat{\omega}, t, \hat{\nu}) + \left(\xi t - \frac{i\hat{\nu}(\hat{\omega} - i\xi \hat{\nu}) \left(1 - \frac{z}{2} \log \frac{z+1}{z-1} \right)}{1 - \frac{i\hat{\nu}}{2} \log \frac{z+1}{z-1}} \right) \mathcal{I}^{[1]}(\xi, \hat{\omega}, t, \hat{\nu}) \right. \\
&\quad \left. - i\hat{\nu} \xi t \left(\frac{1}{t} + \frac{1 - \frac{z}{2} \log \frac{z+1}{z-1}}{1 - \frac{i\hat{\nu}}{2} \log \frac{z+1}{z-1}} \right) \mathcal{I}^{[2]}(\xi, \hat{\omega}, t, \hat{\nu}) \right].
\end{aligned} \tag{A6}$$

Now, in Eq. (A5), before obtaining the second term, note that, $\tilde{n}^i = A^{ij}n^j = n^i - t\hat{k}^i$, and $\tilde{n}^2 = 1 - t^2$.

$$\begin{aligned} \frac{1}{\tilde{n}^2}\tilde{n}^i\Pi^{ij}\tilde{n}^j &= \frac{m_D^2}{1-t^2}\left[-\frac{t^2\hat{\omega}z}{2}f_0(\xi) + \frac{\xi}{2}f_1(\xi) + \frac{1}{2}t^2\hat{\omega}z^2\mathcal{I}^{[0]}(\xi, \hat{\omega}, t, \hat{\nu}) + \frac{1}{2}tz(i\hat{\nu}\xi - 2\hat{\omega} + t^2\xi\hat{\omega})\mathcal{I}^{[1]}(\xi, \hat{\omega}, t, \hat{\nu})\right. \\ &+ \left.\frac{1}{2}(-i(1+t^2)\hat{\nu}\xi + \hat{\omega} - 2t^2\xi\hat{\omega})\mathcal{I}^{[2]}(\xi, \hat{\omega}, t, \hat{\nu}) + \frac{1}{2}\xi t\mathcal{I}^{[3]}(\xi, \hat{\omega}, t, \hat{\nu})\right] + m_D^2\frac{i\hat{\nu}(t-1)}{1-t^2}\frac{2-z\log\frac{z+1}{z-1}}{2-i\hat{\nu}\log\frac{z+1}{z-1}} \\ &\times \left[\frac{\hat{\omega}t}{2}f_0(\xi) - \frac{\hat{\omega}tz}{2}\mathcal{I}^{[0]}(\xi, \hat{\omega}, t, \hat{\nu}) + \frac{\hat{\omega} - \xi t^2z - i\hat{\nu}\xi(1-t^2)}{2}\mathcal{I}^{[1]}(\xi, \hat{\omega}, t, \hat{\nu}) + \frac{\xi t}{2}\mathcal{I}^{[2]}(\xi, \hat{\omega}, t, \hat{\nu})\right]. \end{aligned} \quad (\text{A7})$$

So, Eq. (A5) becomes

$$\begin{aligned} \alpha(\xi, \hat{\omega}, t, \hat{\nu}) &= \frac{m_D^2}{2(1-t^2)}\left[\hat{\omega}zf_0(\xi) - \xi t^2f_1(\xi) + \hat{\omega}(1-t^2-z^2)\mathcal{I}^{[0]}(\xi, \hat{\omega}, t, \hat{\nu}) + t\{\xi(1-t^2) + 2\hat{\omega}z - \xi z^2\}\right. \\ &\times \left.\mathcal{I}^{[1]}(\xi, \hat{\omega}, t, \hat{\nu}) - (\hat{\omega} - 2\xi zt^2)\mathcal{I}^{[2]}(\xi, \hat{\omega}, t, \hat{\nu}) - \xi t\mathcal{I}^{[3]}(\xi, \hat{\omega}, t, \hat{\nu})\right]. \end{aligned} \quad (\text{A8})$$

Now, the structure function $\gamma(\xi, \hat{\omega}, t, \hat{\nu})$ can be obtained as

$$\begin{aligned} \gamma(\xi, \hat{\omega}, t, \hat{\nu}) &= \frac{1}{\tilde{n}^2}\tilde{n}^i\Pi^{ij}\tilde{n}^j - \alpha(\xi, \hat{\omega}, t, \hat{\nu}) \\ &= \frac{m_D^2}{2(1-t^2)}\left[\xi(1+t^2)f_1(\xi) - \hat{\omega}z(1+t^2)f_0(\xi) - \hat{\omega}((1-t^2) - z^2(1+t^2))\mathcal{I}^{[0]}(\xi, \hat{\omega}, t, \hat{\nu})\right. \\ &- t(4\hat{\omega}z - 2\xi z^2 + \xi(1-t^2)(1+\hat{\omega}z))\mathcal{I}^{[1]}(\xi, \hat{\omega}, t, \hat{\nu}) \\ &- \left.(4\xi z - 2\hat{\omega} - \xi(1-t^2)(\hat{\omega} + 3z))\mathcal{I}^{[2]}(\xi, \hat{\omega}, t, \hat{\nu}) + 2\xi t\mathcal{I}^{[3]}(\xi, \hat{\omega}, t, \hat{\nu})\right] \end{aligned} \quad (\text{A9})$$

From Eq. (16), $\rho(\xi, \hat{\omega}, t, \hat{\nu})$ can be written as,

$$\begin{aligned} \rho &= m_D^2\frac{\hat{k}^i\tilde{n}^j}{\tilde{n}^2}\left[\int\frac{d\Omega}{4\pi}v^i\frac{v^l + \xi(\mathbf{v}\cdot\mathbf{n})n^l}{(1+\xi(\mathbf{v}\cdot\mathbf{n})^2)^2}\frac{\delta^{lj}(\hat{\omega} - \hat{\mathbf{k}}\cdot\mathbf{v}) + \hat{k}^l v^j}{\hat{\omega} + i\hat{\nu} - \hat{\mathbf{k}}\cdot\mathbf{v}} + i\hat{\nu}\int\frac{d\Omega'}{4\pi}\frac{v^i}{\hat{\omega} + i\hat{\nu} - \hat{\mathbf{k}}\cdot\mathbf{v}'}\right. \\ &\times \left.\int\frac{d\Omega}{4\pi}\frac{v^l + \xi(\mathbf{v}\cdot\mathbf{n})n^l}{(1+\xi(\mathbf{v}\cdot\mathbf{n})^2)^2}\frac{\delta^{lj}(\hat{\omega} - \hat{\mathbf{k}}\cdot\mathbf{v}) + \hat{k}^l v^j}{\hat{\omega} + i\hat{\nu} - \hat{\mathbf{k}}\cdot\mathbf{v}}\frac{1}{\mathcal{W}(\hat{\omega}, \hat{\nu})}\right] \\ &= \rho_1 + \rho_2, \end{aligned} \quad (\text{A10})$$

with

$$\begin{aligned} \rho_1 &= m_D^2\frac{1}{\tilde{n}^2}\int\frac{d\Omega}{4\pi}(\hat{\mathbf{k}}\cdot\mathbf{v})\frac{v^l + \xi(\mathbf{v}\cdot\mathbf{n})n^l}{(1+\xi(\mathbf{v}\cdot\mathbf{n})^2)^2}\frac{\tilde{n}^l(\hat{\omega} - \hat{\mathbf{k}}\cdot\mathbf{v}) + \hat{k}^l(\tilde{\mathbf{n}}\cdot\mathbf{v})}{\hat{\omega} + i\hat{\nu} - \hat{\mathbf{k}}\cdot\mathbf{v}} \\ &= \frac{m_D^2}{2(1-t^2)}\left[\xi tz\mathcal{I}^{[2]}(\xi, \hat{\omega}, t, \hat{\nu}) - \hat{\omega}tz^2\mathcal{I}^{[0]}(\xi, \hat{\omega}, t, \hat{\nu}) + z(\hat{\omega} - \xi t^2z - i\hat{\nu}\xi(1-t^2))\right. \\ &\times \left.\mathcal{I}^{[1]}(\xi, \hat{\omega}, t, \hat{\nu}) + \hat{\omega}tzf_0(\xi)\right], \end{aligned} \quad (\text{A11})$$

and

$$\begin{aligned} \rho_2 &= \frac{i\hat{\nu}m_D^2}{1-t^2}\int\frac{d\Omega'}{4\pi}\frac{\hat{\mathbf{k}}\cdot\mathbf{v}'}{\hat{\omega} + i\hat{\nu} - \hat{\mathbf{k}}\cdot\mathbf{v}'}\int\frac{d\Omega}{4\pi}\frac{v^l + \xi(\mathbf{v}\cdot\mathbf{n})n^l}{(1+\xi(\mathbf{v}\cdot\mathbf{n})^2)^2}\frac{\tilde{n}^l + (\hat{\omega} - \hat{\mathbf{k}}\cdot\mathbf{v}) + \hat{k}^l(\mathbf{v}\cdot\tilde{\mathbf{n}})}{(\hat{\omega} + i\hat{\nu} - \hat{\mathbf{k}}\cdot\mathbf{v})\mathcal{W}(\hat{\omega}, \hat{\nu})} \\ &= m_D^2\frac{\hat{\omega} - z\mathcal{W}(\hat{\omega}, \hat{\nu})}{2(1-t^2)\mathcal{W}(\hat{\omega}, \hat{\nu})}\left[\hat{\omega}tf_0(\xi) + \xi t\mathcal{I}^{[2]}(\xi, \hat{\omega}, t, \hat{\nu}) - \hat{\omega}tz\mathcal{I}^{[0]}(\xi, \hat{\omega}, t, \hat{\nu}) + (\hat{\omega} - i\hat{\nu}\xi(1-t^2) - \xi, t^2z)\right. \\ &\times \left.\mathcal{I}^{[1]}(\xi, \hat{\omega}, t, \hat{\nu})\right]. \end{aligned} \quad (\text{A12})$$

Combining Eqs. (A11) and (A12), we get

$$\begin{aligned} \rho(\xi, \hat{\omega}, t, \hat{\nu}) &= \frac{\hat{\omega}m_D^2}{2\mathcal{W}(\hat{\omega}, \hat{\nu})(1-t^2)}\left[\hat{\omega}tf_0(\xi) - \hat{\omega}tz\mathcal{I}^{[0]}(\xi, \hat{\omega}, t, \hat{\nu})\right. \\ &+ \left.\{\hat{\omega}(1+\xi - \xi t^2) - \xi z\}\mathcal{I}^{[1]}(\xi, \hat{\omega}, t, \hat{\nu}) + \xi t\mathcal{I}^{[2]}(\xi, \hat{\omega}, t, \hat{\nu})\right]. \end{aligned} \quad (\text{A13})$$

Lastly, we can get the expression of $\delta(\xi, \hat{\omega}, t, \hat{\nu})$ from Eq. (16) as

$$\begin{aligned}
\delta &= m_D^2 \frac{\hat{k}^j \tilde{n}^i}{\tilde{n}^2} \left[\int \frac{d\Omega}{4\pi} v^i \frac{v^l + \xi(\mathbf{v} \cdot \mathbf{n})n^l}{(1 + \xi(\mathbf{v} \cdot \mathbf{n})^2)^2} \frac{\delta^{lj}(\hat{\omega} - \hat{\mathbf{k}} \cdot \mathbf{v}) + \hat{k}^l v^j}{\hat{\omega} + i\hat{\nu} - \hat{\mathbf{k}} \cdot \mathbf{v}} + i\hat{\nu} \int \frac{d\Omega'}{4\pi} \frac{v'^i}{\hat{\omega} + i\hat{\nu} - \hat{\mathbf{k}} \cdot \mathbf{v}'} \right. \\
&\times \left. \int \frac{d\Omega}{4\pi} \frac{v^l + \xi(\mathbf{v} \cdot \mathbf{n})n^l}{(1 + \xi(\mathbf{v} \cdot \mathbf{n})^2)^2} \frac{\delta^{lj}(\hat{\omega} - \hat{\mathbf{k}} \cdot \mathbf{v}) + \hat{k}^l v^j}{\hat{\omega} + i\hat{\nu} - \hat{\mathbf{k}} \cdot \mathbf{v}} \frac{1}{\mathcal{W}(\hat{\omega}, \hat{\nu})} \right] \\
&= \frac{\hat{\omega} m_D^2}{2(1 - t^2)} \left[tz f_0(\xi) - tz^2 \mathcal{I}^{[0]}(\xi, \hat{\omega}, t, \hat{\nu}) + z(1 - \xi t^2) \mathcal{I}^{[1]}(\xi, \hat{\omega}, t, \hat{\nu}) + \xi t \mathcal{I}^{[2]}(\xi, \hat{\omega}, t, \hat{\nu}) \right]. \tag{A14}
\end{aligned}$$

-
- [1] H. A. Weldon, Phys. Rev. D **26**, 1394 (1982).
[2] E. Braaten and R. D. Pisarski, Nucl. Phys. B **337**, 569 (1990).
[3] J. Frenkel and J. C. Taylor, Nucl. Phys. B **334**, 199 (1990).
[4] E. Braaten and R. D. Pisarski, Phys. Rev. D **45**, R1827 (1992).
[5] N. Haque, A. Bandyopadhyay, J. O. Andersen, M. G. Mustafa, M. Strickland, and N. Su, JHEP **05**, 027, arXiv:1402.6907 [hep-ph].
[6] N. Haque and M. G. Mustafa, Prog. Part. Nucl. Phys. **140**, 104136 (2025), arXiv:2404.08734 [hep-ph].
[7] T. Matsui and H. Satz, Phys. Lett. B **178**, 416 (1986).
[8] E. Eichten, K. Gottfried, T. Kinoshita, J. B. Kogut, K. D. Lane, and T.-M. Yan, Phys. Rev. Lett. **34**, 369 (1975), [Erratum: Phys.Rev.Lett. **36**, 1276 (1976)].
[9] E. Eichten, K. Gottfried, T. Kinoshita, K. D. Lane, and T.-M. Yan, Phys. Rev. D **17**, 3090 (1978), [Erratum: Phys.Rev.D **21**, 313 (1980)].
[10] E. Eichten, K. Gottfried, T. Kinoshita, K. D. Lane, and T.-M. Yan, Phys. Rev. D **21**, 203 (1980).
[11] W. Buchmuller and S. H. H. Tye, Phys. Rev. D **24**, 132 (1981).
[12] Y. Koma, M. Koma, and H. Wittig, Phys. Rev. Lett. **97**, 122003 (2006), arXiv:hep-lat/0607009.
[13] N. Brambilla, A. Pineda, J. Soto, and A. Vairo, Rev. Mod. Phys. **77**, 1423 (2005), arXiv:hep-ph/0410047.
[14] F. Karsch, D. Kharzeev, and H. Satz, Phys. Lett. B **637**, 75 (2006), arXiv:hep-ph/0512239.
[15] S. Chatrchyan *et al.* (CMS), Phys. Rev. Lett. **107**, 052302 (2011), arXiv:1105.4894 [nucl-ex].
[16] S. Chatrchyan *et al.* (CMS), Phys. Rev. Lett. **109**, 222301 (2012), [Erratum: Phys.Rev.Lett. **120**, 199903 (2018)], arXiv:1208.2826 [nucl-ex].
[17] V. Agotiya, V. Chandra, and B. K. Patra, Phys. Rev. C **80**, 025210 (2009), arXiv:0808.2699 [hep-ph].
[18] P. Romatschke and M. Strickland, Phys. Rev. D **68**, 036004 (2003), arXiv:hep-ph/0304092.
[19] P. Romatschke and M. Strickland, Phys. Rev. D **70**, 116006 (2004), arXiv:hep-ph/0406188.
[20] S. Mrowczynski, A. Rebhan, and M. Strickland, Phys. Rev. D **70**, 025004 (2004), arXiv:hep-ph/0403256.
[21] S. Mrowczynski, B. Schenke, and M. Strickland, Phys. Rept. **682**, 1 (2017), arXiv:1603.08946 [hep-ph].
[22] P. Romatschke and A. Rebhan, Phys. Rev. Lett. **97**, 252301 (2006), arXiv:hep-ph/0605064.
[23] A. Dumitru, Y. Guo, and M. Strickland, Phys. Rev. D **79**, 114003 (2009), arXiv:0903.4703 [hep-ph].
[24] A. Dumitru, Y. Guo, and M. Strickland, Phys. Lett. B **662**, 37 (2008), arXiv:0711.4722 [hep-ph].
[25] Y. Burnier, M. Laine, and M. Vepsalainen, Phys. Lett. B **678**, 86 (2009), arXiv:0903.3467 [hep-ph].
[26] A. Dumitru, Y. Guo, A. Mocsy, and M. Strickland, Phys. Rev. D **79**, 054019 (2009), arXiv:0901.1998 [hep-ph].
[27] L. Thakur, N. Haque, U. Kakade, and B. K. Patra, Phys. Rev. D **88**, 054022 (2013), arXiv:1212.2803 [hep-ph].
[28] L. Dong, Y. Guo, A. Islam, A. Rothkopf, and M. Strickland, JHEP **09**, 200, arXiv:2205.10349 [hep-ph].
[29] R. Zhao, L. Qiu, Y. Guo, and M. Strickland, Phys. Rev. D **108**, 034023 (2023), arXiv:2306.12851 [hep-ph].
[30] M. E. Carrington, T. Fugleberg, D. Pickering, and M. H. Thoma, Can. J. Phys. **82**, 671 (2004), arXiv:hep-ph/0312103.
[31] B. Schenke, M. Strickland, C. Greiner, and M. H. Thoma, Phys. Rev. D **73**, 125004 (2006), arXiv:hep-ph/0603029.
[32] A. Kumar, M. Y. Jamal, V. Chandra, and J. R. Bhatt, Phys. Rev. D **97**, 034007 (2018), arXiv:1709.01032 [nucl-th].
[33] L. Thakur, U. Kakade, and B. K. Patra, Phys. Rev. D **89**, 094020 (2014), arXiv:1401.0172 [hep-ph].
[34] J. Sebastian, L. Thakur, H. Mishra, and N. Haque, Phys. Rev. D **108**, 094001 (2023), arXiv:2308.04410 [hep-ph].
[35] B. Singh, L. Thakur, and H. Mishra, Phys. Rev. D **97**, 096011 (2018), arXiv:1711.03071 [hep-ph].
[36] L. Thakur, N. Haque, and H. Mishra, Phys. Rev. D **95**, 036014 (2017), arXiv:1611.04568 [hep-ph].
[37] J. Sebastian, M. Y. Jamal, and N. Haque, Phys. Rev. D **107**, 054040 (2023), arXiv:2207.08510 [hep-ph].
[38] Q. Du, A. Dumitru, Y. Guo, and M. Strickland, JHEP **01**, 123, arXiv:1611.08379 [hep-ph].
[39] L. Thakur, N. Haque, and Y. Hirono, JHEP **06**, 071, arXiv:2004.03426 [hep-ph].
[40] X. Wang and I. Shovkovy, Phys. Rev. D **104**, 056017 (2021), arXiv:2103.01967 [nucl-th].
[41] H. A. Weldon, Phys. Rev. D **42**, 2384 (1990).